Biomedicine & Pharmacotherapy 81 (2016) 225–234

Available online at
ScienceDirect
www.sciencedirect.com

Elsevier Masson France
EM|consulte
www.em-consulte.com/en

Effects of nitric oxide system and osmotic stress on Aquaporin-1 in the postnatal heart

Vanina A. Netti[a,*], Agustina N. Iovane[a], Mariana C. Vatrella[a], Elsa Zotta[b], Andrea L. Fellet[a], Ana M. Balaszczuk[a]

[a] Cátedra de Fisiología, Facultad de Farmacia y Bioquímica, Universidad de Buenos Aires, IQUIMEFA-CONICET, Junín 956, Buenos Aires, Argentina
[b] Laboratorio de Fisiopatogenia, Facultad de Medicina, Universidad de Buenos Aires, Paraguay 2155, Buenos Aires, Argentina

ARTICLE INFO

Article history:
Received 1 February 2016
Received in revised form 31 March 2016
Accepted 31 March 2016

Keywords:
Aquaporin-1
Dehydration
Heart
Nitric oxide
Postnatal growth

ABSTRACT

Aquaporin-1 (AQP1) is expressed in the heart and its relationship with NO system has not been fully explored. The aims of this work were to study the effects of NO system inhibition on AQP1 abundance and localization and evaluate AQP1 S-nitrosylation in a model of water restriction during postnatal growth. Rats aged 25 and 50 days ($n = 15$) were divided in: R: water restriction; C: water *ad libitum*; RL: L-NAME (4 mg/kg day) + water restriction; CL: L-NAME + water *ad libitum*. AQP1 protein levels, immunohistochemistry and S-nitrosylation (colocalization of AQP1 and S-nitrosylated cysteines by confocal microscopy) were determined in cardiac tissue. We also evaluated the effects of NO donor sodium nitroprusside (SNP) on osmotic water permeability of cardiac membrane vesicles by stopped-flow spectrometry. AQP1 was present in cardiac vascular endothelium and endocardium in C and CL animals of both ages. Cardiac AQP1 levels were increased in R50 and RL50 and appeared in cardiomyocyte plasma membrane. No changes in AQP1 abundance or localization were observed in R25, but RL25 group showed AQP1 presence on cardiomyocyte sarcolemma. AQP1 S-nitrosylation was increased in R25 group, without changes in the 50-day-old group. Cardiac membrane vesicles expressing AQP1 presented a high water permeability coefficient and pretreatment with SNP decreased water transport. Age-related influence of NO system on AQP1 abundance and localization in the heart may affect cardiac water homeostasis during hypovolemic state. Increased AQP1 S-nitrosylation in the youngest group may decrease osmotic water permeability of cardiac membranes, having a negative impact on cardiac water balance.

1. Introduction

Aquaporins (AQPs) are a family of water channel proteins that allow the rapid transport of water across the plasma membrane in response to osmotic gradients [1]. In the rat heart, Aquaporin-1 (AQP1) is the AQP that determines water transport, as cardiomyocyte membrane water permeability was significantly reduced only in the absence of AQP1 [2]. AQP1 has been linked to cardiovascular homeostasis in many pathological conditions, such as myocardial edema and ischemia; however, its physiological role still has not been determined in the heart [3].

Several AQPs have been reported to facilitate the transport of small solutes, such as carbon dioxide or ammonia [4,5]. Herrera et al. [6] demonstrated that AQP1 transports nitric oxide (NO), a well-known regulator of cardiovascular function. They also described the physiological relevance of NO transport out of endothelial cells and into vascular smooth muscle mediated by AQP1 [7]. Even though solute transport by AQPs still remains controversial [8–10], it has been proposed that the central pore conformed by the four monomers of AQP1 may build the hydrophobic pathway that allows the transport of gas molecules [11]. Additionally, focusing on NO system, it has also been reported that NO is involved in regulation of AQPs abundance and trafficking. Previous results from our laboratory in renal tissue indicated that NO system decreased AQP2 expression levels and its apical localization during hypovolemic state [12]. Moreover, it has been described that NO also affects AQP5 membrane insertion in epithelial pulmonary cells [13]. Changes in AQPs localization or abundance are likely to modulate changes in cell volume in response to an anisosmotic environment. However, the effects of NO system on AQP1 regulation *in vivo* have not been fully studied, particularly in the heart.

A well-known mechanism by which NO regulates protein function and cellular physiology is protein S-nitrosylation. The

* Corresponding author.
E-mail address: vnetti@conicet.gov.ar (V.A. Netti).

http://dx.doi.org/10.1016/j.biopha.2016.03.050
0753-3322/

formation of S-nitrosothiols (SNO) occurs when the thiol group of protein cysteine residues (Cys) reacts with NO [14]. It has been described that S-nitrosylation of several channels is involved in permeability regulation [15]. Moreover, it has been reported that water deprivation significantly enhanced the expression of S-nitrosylated proteins the rat brain [16]. However, S-nitrosylation of AQP1 and the effects of this posttranslational modification on water permeability have not been studied in the heart.

On the other hand, dehydration represents a significant problem in the pediatric population, being one of the main causes of mortality in children. During postnatal growth, an inadequate hydration may have cardiovascular consequences in adulthood. However, age-related clinical consequences of dehydration in the heart have not been fully explored in infants. In previous work done in our laboratory, we demonstrated that cardiovascular AQP1 abundance and localization can be differentially regulated in response to osmotic stress induced by water restriction during postnatal life [17]. We also reported that NO system participates in cardiovascular adaptation to hypovolemia *in vivo* and this response also depends on postnatal age [18]. Considering the mentioned age-related changes in AQP1 and NO system during osmotic stress and that the relationship between AQP1 and NO in the heart still remains to be explored, the aims of the present work were in rats aged 25 and 50 days: 1) To study the effects of NO system inhibition on AQP1 localization and protein levels *in vivo*; 2) To evaluate AQP1 S-nitrosylation during hypovolemic state and its consequences on water permeability.

2. Materials and methods

2.1. Animals

Male Sprague-Dawley rats were obtained from the breeding laboratories of the School of Pharmacy and Biochemistry (University of Buenos Aires, Argentina). Newborn rats were maintained with their dam until day 21 (weaning age). When they reached the age of 25 and 50 days, the animals were housed individually in metabolic cages with an automatic light/dark cycle of 12 h/12 h and fed with standard rat chow from nutriments Purina (Buenos Aires, Argentina) and tap water *ad libitum* until the beginning of the experimental period, in order to adapt to the new environment. All study protocols were reviewed and approved by the National Administration of Medicine, Food and Medical Technology, Department of Health and Environment of the Nation, Argentina (N° 6344-96).

2.2. Experimental protocol

Male Sprague-Dawley rats aged 25 and 50 days were randomly assigned as follows ($n = 15$ each group):

2.2.1. C group

Animals had continuous access to both food and water during the 3-day experimental period, representing a normohydrated group of rats.

2.2.2. CL group

Animals received a continuous infusion of L-NAME (NOS unspecific inhibitor) via ALZET osmotic mini pumps and had continuous access to both food and water during the 3-day experimental period.

2.2.3. R group

Rats were deprived of water for 72 h but had continuous access to food.

2.2.4. RL group

Rats received a continuous infusion of L-NAME via ALZET osmotic mini pumps and were deprived of water for 72 h.

L-NAME dosage (4 mg/kg day) did not increase blood pressure (BP) [19]. In order to verify this, systolic BP (SBP) and NOS activity were measured in both age groups. For osmotic mini-pump implantation (model 1003D), animals were submitted to a brief surgery: they were anesthetized with light ether anesthesia and pumps were implanted subcutaneously between the scapulae using aseptic technique. Animals were allowed to recover for 24 h before the beginning of the experiments. L-NAME infusion was prepared with sterile saline, filtered and inserted in mini-pumps in a laminar flow cabinet in order to avoid contamination. Control animals were infused with sterile saline.

At the end of each experimental period and with the purpose of validating that water restriction established a dehydration status, body weight was determined and blood collections were made to determinate hematocrit (from duplicate blood-filled hematocrit tubes), natremia (ion-selective analyzer t-410, Tecnolab) and plasma osmolarity (microosmometer losmette TM).

2.3. Systolic blood pressure

SBP was indirectly measured in awaken animals by the tail- cuff method using a PowerLab data acquisition system device and LabChart software (AD Instruments). Prior to measuring SBP, rats were warmed in a thermostated silent room for 30 min. The SBP value for each rat was calculated as the average of five separate measurements at each session.

2.4. NOS activity

NO system activity in cardiac tissue was assessed by measuring the conversion of [^{14}C]- L-Arginine to [^{14}C]-L-Citrulline. 50 μg of protein of homogenized tissues were incubated in Tris-HCl buffer (pH = 7.4) containing 1 mg/ml of L-Arginine, [^{14}C] L- Arginine (346 mCi/mL), L-valine (67 mM), NADPH (1 mM), calmodulin (30 nM), tetrahydrobiopterin (5 μM) y $CaCl_2$ (2 mM) for 1 h at room temperature. Negative controls were performed by adding 10 mM L-NAME (NOS unspecific inhibitor) to reaction medium. At the end of the incubation period, reaction was arrested by adding HEPES-EDTA solution (pH = 5.5) at 0 °C. Reaction mixtures were loaded into cation exchange columns (Dowex AG 50W-X8, Na^+ form; Bio-Rad) and [^{14}C]-L-citrulline was eluted from columns with 1 mL of ddH_2O. The amount of [^{14}C]-L-citrulline eluted was quantified using a liquid scintillation counter (Wallac 1414 WinSpectral; EG&G, Finland). All compounds, except [U^{14}C]-L-Arginine monohydrochloride (346 mCi/mmol, Amersham Life Science), were purchased from Sigma Chemicals. Total protein levels were determined by the Lowry method, using bovine serum albumin as a standard.

2.5. Cardiomyocyte diameter

Cardiac tissue from all groups of animals were fixed in phosphate-buffered 10% formaldehyde (pH 7.2) and embedded in paraffin using conventional histological techniques. Paraffin sections were cut at 4 μm with a microtome (Leica RM 2125, Wetzlar, Germany), deparaffined, rehydrated and stained with hematoxylin. Sections were analyzed using an Olympus BX51 light microscope equipped with a digital camera (Qcolor 3 Olympus America Inc., Canada) and connected to the Image-Pro Plus software. The major and minor diameters of cardiomyocytes were measured using Q Capture Pro software in 4-μm thick cross-sections of the heart at x400 magnification. Cardiomyocytes chosen to be measured had central and nearly round shape nuclei.

Afterward, major and minor diameters were averaged to obtain mean cardiomyocyte diameter.

2.6. AQP1 immunohistochemistry

Deparaffinized and rehydrated sections were used to study AQP1 localization in the heart. First, endogenous peroxidase activity was blocked by treating with 0.5% H_2O_2 in methanol for 30 min. AQP1 was detected using a rabbit antibody at a dilution of 1:500 (H-55, Santa Cruz Biotechnologies). Immunostaining was carried out using a commercially modified avidin–biotin–peroxidase complex technique, Vectastain ABC kit (Universal Elite, Vector Laboratories) and counterstained with hematoxylin. The sections were observed by light microscopy (Nikon Eclipse 200). Images were acquired by using Nikon Digital SIGHT D5-Fi1 and NIS Elements-F 3.0 software. Negative controls were performed by omitting primary antibody.

2.7. Western blot

Left ventricle was disrupted on ice using a tissue homogenizer (Omni International) in buffer containing 50 mM Tris, 0.1 mM EDTA, 0.1 mM EGTA, 1% Triton, 1 mM PMSF, 1 μM pepstatin, 2 μM leupeptin, 1X protease inhibitor cocktail (Roche Diagnostics). Protein concentration was determined by Lowry assay. Equal amounts of protein (50–75 μg protein/lane) of pooled samples (because of small amount of ventricular tissue in 25-day-old rats) were separated by electrophoresis in 12% SDS– polyacrylamide gels (Bio-Rad), transferred to a nitrocellulose membrane (Bio-Rad) and blocked with 5% nonfat milk. Membranes were incubated with a rabbit antibody against AQP1 at a dilution 1:500 (H-55, Santa Cruz Biotechnologies) and a goat anti-rabbit antibody conjugated with HSP at a dilution 1:6000 ((170-6515, Bio-Rad). Samples were revealed by chemiluminescence using ECL reagent for 2–4 min. Blots were then stripped with NaOH 0,2 M and re-incubated with a rabbit antibody against β-actin at a dilution 1:2000 (BD, Biosciences). Bands were quantified by densitometry scanning using a Hewlett-Packard scanner and gel analyzer tools of Image J software (NIH). Each western blot was made by triplicate. Protein levels were expressed as a ratio of the optical densities of the AQP1 and β-actin band to detect inaccuracies in protein loading.

2.8. Cardiac water content

The hearts of animals from all the experimental groups were extracted and weighted. Later, with the objective of dehydrating the hearts, they were placed into a stove at a temperature of 80 °C (Dalvo Instruments, Embiotec SRL) and weighted daily until they reached constant weight. Cardiac water content was calculated following the formula of Ding et al. [20].

2.9. S-nitrosylation of AQP1

Deparaffinized and rehydrated tissue sections were used for AQP1 and nitrosylated Cys (SNO-Cys) detection by immunofluorescence and confocal microscopy. Blocking of unspecific binding sites was performed by incubation with BSA 5% and 0,2% triton X-100 pH = 7.4 1 h at room temperature. For AQP1 detection, a mouse antibody (sc-32737, Santa Cruz Biotechnologies) was used at a dilution of 1/50 overnight at 4 °C. SNO-Cys were detected by using a rabbit antibody (Abcam ab50185) at a dilution of 1/100 in the same conditions. Antibody specificity was tested by pre-incubating the samples with DTT 15 mM, which disrupts SNO bond. Secondary antibodies employed were a goat anti-mouse IgG-FITC antibody (sc-2010, Santa Cruz Biotechnologies) and a goat anti-rabbit IgG-Rhodamine antibody (AP307R, Chemicon, EMD Millipore) at dilutions of 1/100 for 2 h at room temperature. Images were acquired by using confocal microscope Nikon C1 and EZ-C1 FreeViewer software at 600X. Images were analyzed for colocalization of both signals by using WCIF ImageJ software.

2.10. Osmotic permeability of cardiac membranes

Whole hearts of normal rats were pooled and homogenized and the membrane fraction was obtained first by ultracentrifugation and then by sucrose gradient centrifugation. Cardiac tissue membrane vesicles were formed by forcing the obtained membrane fractions though a 27 G needle 20 times, as previously described [2]. The presence of AQP1 in vesicles was assessed by Western Blotting (as described in section 2.7). Vesicle size and morphology was assessed by dynamic light scattering (DLS) using a Zetasizer Nano-Zs (Malvern Instruments, UK) with a He-Ne laser (633 nm) and a digital correlator ZEN3600. Measurements of vesicle size were carried out in membranes submitted to the same dilution protocol as those used in stopped-flow measurements. Electron micrographs were also used to determine vesicle diameters by transmission electron microscope Zeiss model EM-109T equipped with a digital camera Gatan ES1000W. Samples were examined at x50000.

Water permeability measurements to obtain the osmotic water permeability coefficient (*Pf*) were performed in a stopped-flow spectrofluorimeter (Applied Photophysics), where equal volumes of vesicles and a hyperosmotic medium (Sucrose 400 mOsm) were mixed and the kinetics of vesicle volume changes induced by an outward water flow was followed by light scattering at 500 nm. Experiments were performed in control conditions and pre-incubating the vesicles with 100 μM $HgCl_2$ (a known inhibitor of AQPs) and 1 mM sodium nitroprusside (SNP), a NO donor. Data was fitted to double-exponential functions using GraphPad software and *Pf* was calculated as previously described [21].

2.11. Statistical analysis

Data in tables and figures are expressed as mean values ± SD. Data were evaluated with one-way analysis of variance (ANOVA) and Tukey's post hoc test for multiple comparisons was used. Normal distribution was assessed by using the Shapiro-Wilk test and the Levene's test was used to evaluate the homogeneity of variances. When data distribution was not normal, non-parametric Kolmogórov-Smirnov test was applied. When SD presented statistically significant differences, Tamhane's T2 test was used for post hoc comparisons. All statistical procedures were performed using SPSS statistical software package release 16.0 version.

3. Results

3.1. Validation of the experimental model of NO system inhibition during water restriction

First, with the aim of validating that L-NAME treatment at a subpressor dosage (4 mg/kg day) inhibited NOS activity without a significant increase of BP, SBP and NOS activity were determined. Additionally, in order to evaluate if water restriction protocol induced a dehydration state, body weight and hematocrit, natremia and plasma osmolarity were determined. We also determined heart weight and cardiomyocyte diameter in dehydrated and L-NAME treated rats.

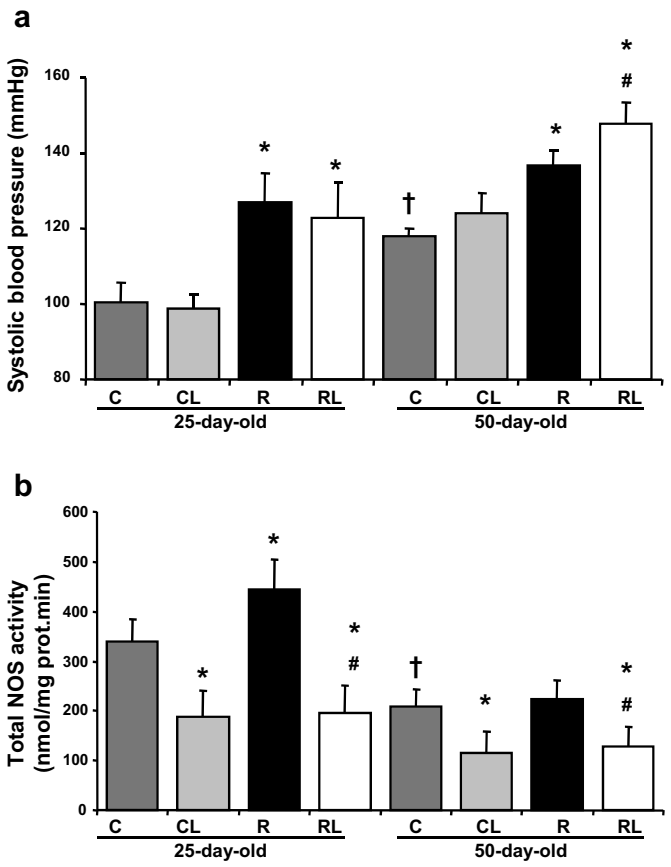

Fig. 1. Validation of experimental model of NO system inhibition at a subpressor dose. Panel A: Systolic blood pressure of 25- and 50-day-old rats ($n = 12$ each group). Data are expressed as mean ± SD. *$p < 0.01$ versus respective C; #$p < 0.01$ versus respective R; †$p < 0.01$ versus 25-day-old rats. Panel B: Cardiac total NOS activity in 25- and 50-day-old ($n = 5$ each group). Data are expressed as mean ± SD. *$p <$ 0.01 versus respective C; †$p < 0.01$ versus 25-day-old rats.

3.1.1. SBP and NOS activity

Results are shown in Fig. 1. NOS inhibition did not modify SBP in control animals of both age groups. Dehydrated rats of both age groups presented an increase in SBP, being this increase larger for the youngest group, as previously reported [18]. In 25-day-old group submitted to water restriction, L-NAME treatment did not modify SBP in comparison to R group, however, the 50-day-old RL group, SBP was higher in RL group in comparison to R. On the other hand, cardiac NOS activity of CL and RL groups of both age groups were decreased by 50% after L-NAME treatment, each compared to its control group. 25-day-old dehydrated rats presented an increase in NOS activity, but no changes were observed in the oldest group in response to water restriction, as previously described [18]. This implicates that L-NAME treatment was efficient to inhibit cardiac NOS in both experimental age groups without increasing SBP.

3.1.2. General features of dehydrated and L-NAME treated animals

L-NAME treatment did not modify the changes in body weight, hematocrit, natremia and plasma osmolarity induced by water restriction in animals of both ages, as shown in Table 1. Moreover, L-NAME treatment did not modify heart weight in both age groups. However, mean cardiomyocyte diameter, which was decreased in dehydrated 25-day-old rats, was similar to control group in RL25 group. 50-day-old rats did not show differences in this parameter during water restriction or L-NAME treatment. Additionally, NOS inhibition did not alter cardiac morphology in both age groups, evaluated by Thricrome staining (data not shown).

3.2. Cardiac AQP1 during osmotic stress: effects of NO system inhibition

3.2.1. Immunohistochemical staining of AQP1 in the heart

With the aim of evaluating cardiac AQP1 localization during L-NAME treatment, an immunohistochemichal staining of the heart was performed. Results are shown in Fig. 2. In control animals of 25 and 50 days of age, AQP1 was present in the endocardium and endothelial cells of capillary and venules, but it was absent in small arterials, being this pattern similar in L-NAME treated animals of both age groups. In the left ventricle of 25-day-old pups, it was observed that NOS inhibition did not modify AQP1 localization in CL group in comparison to group C; however, in the RL group, this protein was present in cardiomyocyte plasma membrane. In the 50-day-old rats, CL group did not show any differences in the localization of this water channel, meanwhile, the R and RL groups showed plasma membrane localization of AQP1.

3.2.2. Cardiac AQP1 protein levels

AQP1 protein levels were higher in 25-day-old pups in comparison to the 50-day-old group, as previously reported [17]. In the left ventricle of 25-day-old pups, no changes in

Table 1
General features of dehydrated and L-NAME treated rats.

	25-day-old rats				50-day-old rats			
	C	CL	R	RL	C	CL	R	RL
Body weight (g)	85 ± 10	90 ± 7	56 ± 6*	57 ± 6*	248 ± 11†	237 ± 12	176 ± 11*	189 ± 6*
Hematocrit (%)	42 ± 2	43 ± 2	55 ± 3*	54 ± 2*	48 ± 2†	48 ± 3	62 ± 2*	61 ± 3*
Natremia (mEq/L)	137 ± 2	139 ± 3	147 ± 3*	150 ± 5*	139 ± 1	138 ± 3	146 ± 3*	146 ± 4*
Plasma Osm (mOsm)	315 ± 6	319 ± 9	347 ± 4*	356 ± 10*	320 ± 8	318 ± 9	359 ± 10*	340 ± 9*
Heart weight (g/100 g bw)	0.48 ± 0.03	0.50 ± 0.06	0.52 ± 0.06	0.49 ± 0.04	0.32 ± 0.06†	0.32 ± 0.04	0.38 ± 0.07	0.36 ± 0.04
Cardiomyocyte diameter (μm)	15.0 ± 1.2	15.4 ± 1.9	13.0 ± 0.8*	15.1 ± 1.6#	17.8 ± 0.8†	16.6 ± 1.3	17.1 ± 1.7	16.0 ± 1.8

Results are expressed as mean ± SD.
Bw: body weight.
* $p < 0.001$ vs. respective C.
# $p < 0.001$ vs. respective R.
† $p < 0.001$ vs. C25.

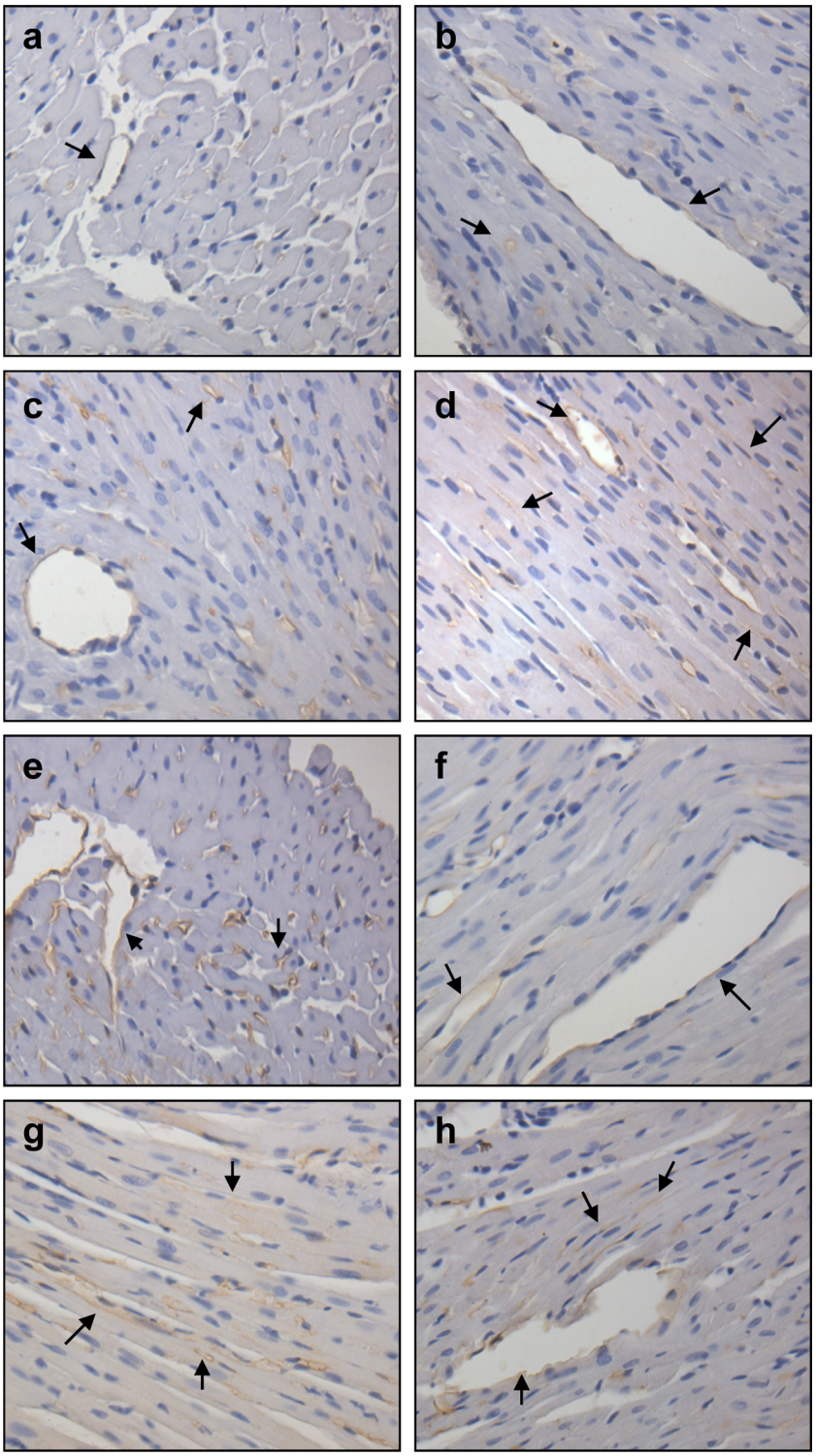

Fig. 2. Immunohistochemical staining of AQP1 in cardiac tissue from 25- and 50-day-old rats ($n = 4$). Arrows indicate positive staining for AQP1. A–D: Representative photographs of the heart of 25-day-old animals from experimental groups C, CL, R and RL respectively. Panels A, B and C: AQP1 in the endocardium and endothelial cells of cardiac capillaries and venues (arrows). Panel D: AQP1 in cardiomyocyte membrane in RL group (arrows). E–H: Representative photographs of the heart of 50-day-old animals from experimental groups C, CL, R and RL respectively. Panels A and B: AQP1 in the endocardium and endothelial cells of cardiac capillaries and venues (arrows). Panel C and D: AQP1 in cardiomyocyte membrane in R and RL groups (arrows). All photographs are X400.

AQP1 protein levels were observed during L-NAME treatment or water restriction. However, in the 50-day-old group, AQP1 was decreased in response to NO system inhibition in control animals. Both groups submitted to water restriction (R and RL) had increased levels of AQP1 when compared to their control group. Results are shown in Fig. 3.

3.2.3. Cardiac water content

Results of cardiac water content are shown in Fig. 4. In the 25-day old group, water restriction induced a decrease in water content in comparison to C and CL groups. However, in RL animals, it was observed that NOS inhibition reversed the effects of water restriction. On the other hand, in the 50-day-old group, no

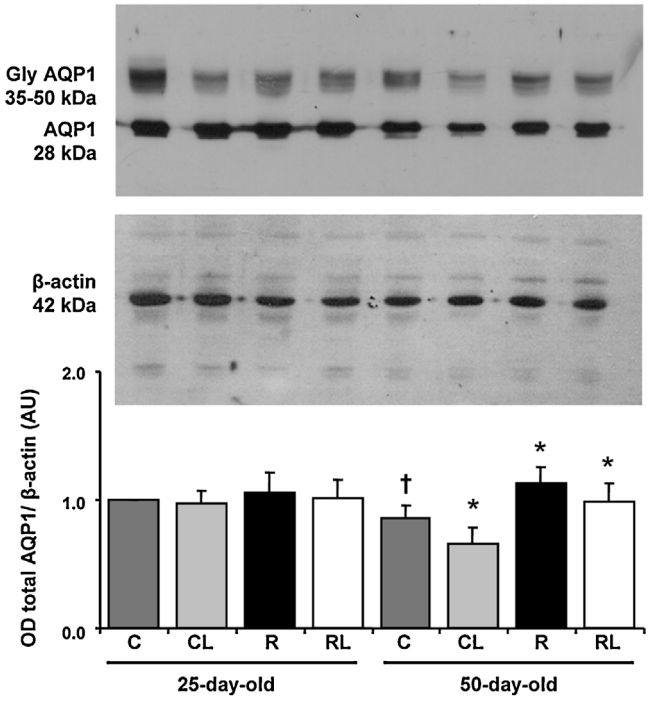

Fig. 3. Representative western blots of AQP1 in the left ventricle from 25- and 50-day-old rats ($n = 6$). Histograms the ratio between mean total AQP1 and β-actin protein levels. Data are expressed as mean ± SD. *$p < 0.01$ versus respective C; †$p < 0.01$ versus 25-day-old.

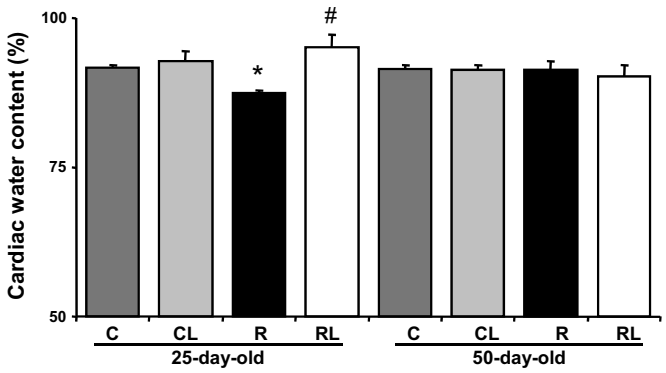

Fig. 4. Cardiac water content (%) (n = 5). Data are expressed as mean ± SD. *$p < 0.05$ vs. C; #$p < 0.05$ vs. R.

differences were observed in cardiac water content after L-NAME treatment or water restriction.

3.3. AQP1 S-nitrosylation and effects of NO donors on Pf of cardiac membranes

With the aim of determining if there was a relationship between the observed the age-related changes in NOS activity and AQP1, we also studied AQP1 S-nitrosylation by colocalization of AQP1 and SNO—Cys fluorescent signals by confocal microscopy during hypovolemic state in rats aged 25 and 50 days. Next, we studied the effects of S-nitrosylation induced by NO donor SNP on cardiac membranes osmotic water permeability by stopped-flow spectrometry.

3.3.1. AQP1 S-nitrosylation

Fig. 5 shows that AQP1 and SNO-Cys staining colocalization was increased in R25 group, whereas there were no significant differences in colocalization of fluorescent signals between control and water-restricted 50-day-old animals. Pre-incubation with DTT 15 mM or L-NAME infusion *in vivo* (4 mg/kg day) caused a significant reduction in Cys-SNO fluorescent signals (Supplementary Fig. 1).

3.3.2. Water permeability measurements

The size and morphology of cardiomyocyte membrane vesicles were assessed by DLS and ME. Table 2 shows the mean diameter of vesicles obtained by DLS for each treatment. Results indicate that vesicles submitted to the different treatments were homogeneous in size without differences in the mean diameter of the main peak of each of them. Similar results were obtained by measuring vesicle diameters by ME, where vesicle morphology could also be evaluated, as it can be observed in Fig. 6. AQP1 presence in vesicles was not affected by the different treatments applied, as it can be observed in Fig. 6. The osmotic water permeability (*Pf*) of heart plasma membrane vesicles was measured after rapidly increasing the extravesicular osmolarity (sucrose 400mOsm) by mixing equal volumes of vesicles and hyperosmotic media using stopped-flow technique and recording the light-scattering signal at 500 nm. Vesicles in control conditions presented a high osmotic water permeability coefficient (*Pf*: 326 ± 17 μm/s, $n = 6$). $HgCl_2$ treatment caused a 30% decrease of water flow across vesicles (Pf: 221 ± 9 μm/s, $n = 4$). Pre-incubation with NO donor, SNP, decreased Pf ever more (*Pf*: 102 ± 4 μm/s, $n = 5$). Vesicle treatment with $HgCl_2$ and SNP showed Pf similar to Hg^{2+} treatment. Fig. 7 shows the time course of light scattering for the different treatments, fast velocity constant and *Pf* values for each treatment.

4. Discussion

The relationship between NO system and AQP1 still remains controversial and has not been fully explored in the heart. Considering that we have previously reported that both AQP1 and NO system participate on cardiovascular adaptation to osmotic stress during postnatal growth [17,18], the present work was designed to study the relationship between NO system and cardiac AQP1 during hypovolemic state in growing rats, as well as AQP1 S-nitrosylation and its effects on osmotic water permeability of cardiac membranes. Initially, we evaluated the effects of NO system inhibition on SBP and NOS activity in order to validate our experimental model. L-NAME treatment of 4 mg/kgday administered by osmotic mini pumps did not change BP significantly in animals from CL group in comparison to C group of both ages, as it was expected. On the other hand, NOS activity indicated that L-NAME treatment was efficient to inhibit enzyme activity by approximately 50% in comparison to the respective control groups of each age. We also verified that water restriction protocol induced a dehydration state by evaluating body weight and hematocrit, natremia and plasma osmolarity, as previously reported [17]. L-NAME treatment did not affect these parameters in animals of both age groups. Altogether, these results allowed us to validate our experimental model. When evaluating SBP in dehydrated rats, the obtained results indicate that L-NAME treatment induced a larger increase in this parameter in the 50-day-old RL group (25%) in comparison to the R group (17%), when comparing them to control animals. This implicates that NO system may participate in BP regulation in the 50-day-group, probably counterbalancing the effects of vasoconstrictor mediators that are released during hypovolemic state (angiotensin II, vasopressin, cathecolamines, among others). However, in the youngest group, this difference was not observed with L-NAME treatment, suggesting that age-related changes during postnatal

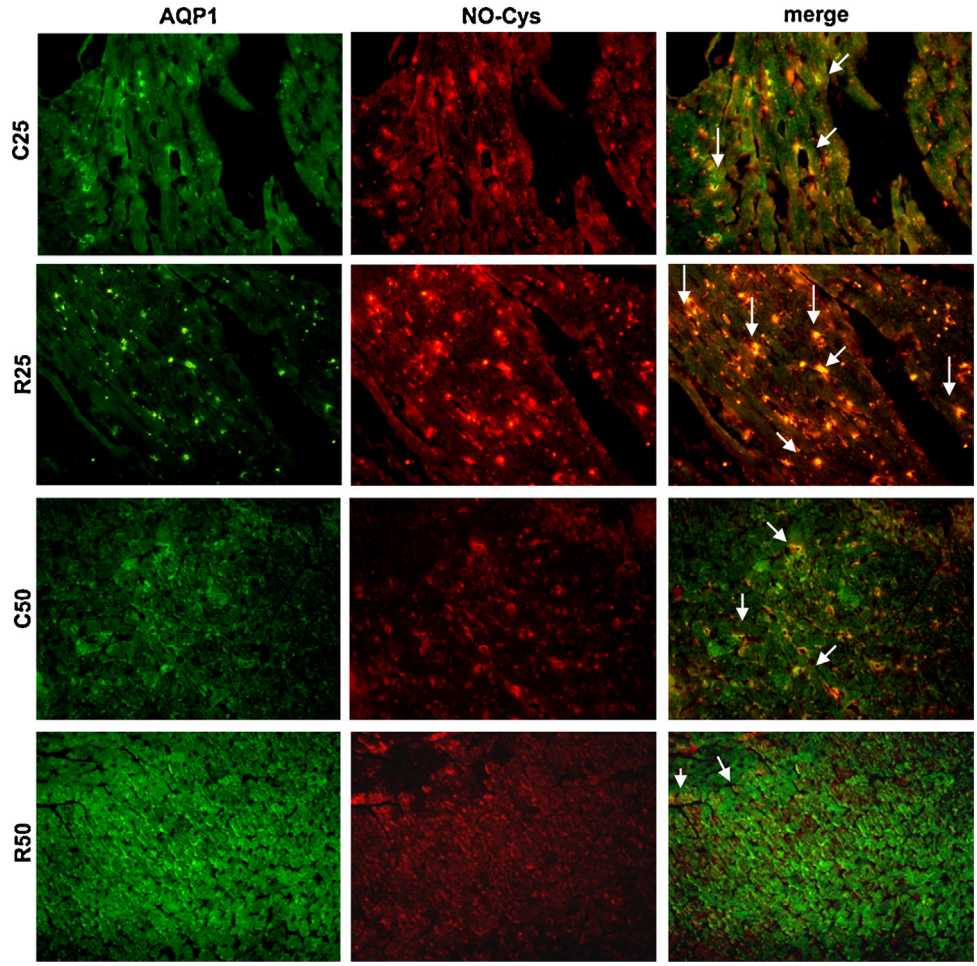

Fig. 5. AQP1 S-nitrosylation by colocalization of fluorescent signals of AQP1 and nitrosylated Cys during hypovolemic state in 25- and 50-day-old rats (n = 4). White arrows indicate colocalization. All photographs are X600.

growth in NO production *in vivo* during hypovolemic state are involved in BP regulation.

In order to study the effects of NOS inhibition on AQP1 localization and abundance *in vivo*, an immunohistochemical staining and western blot were performed in ventricular tissue. Plasma membrane localization of AQP1 was increased in dehydrated 25-day-old RL pups, despite the fact that its protein levels were not increased. This suggests that NO would prevent AQP1 localization in the sarcolemma, which has also been reported for other AQPs, such as AQP5 in the lung [13]. Moreover, increased AQP1 in cardiomyocyte plasma membrane during NO system inhibition is associated to higher cardiac water content and the maintenance of cellular dimensions in RL group in comparison to R group in 25-day-old pups. We propose that, under osmotic stress conditions for 72 h, this increase in cardiac AQP1 plasma membrane may be involved in long-term cell volume regulation. When cells are under hypertonicity conditions, they lose water as the extracellular space and blood have increased osmolality. When this stress is permanent, cells decrease their volume as a consequence of water loss. It has been reported that cells in chronic hypertonicity conditions synthesize osmotically active solutes to retain water with the aim of increasing intracellular osmolality [22]. Increased AQP1 plasma membrane expression in this context may provide a rapid pathway for water influx and possibly contribute to cell volume regulation under these extreme conditions [17]. In line with this, Conner et al. [23] reported that changes in AQP1 subcellular localization in astrocytes regulate changes in cell volume in response to a hypotonic environment. On the other hand, during postnatal growth, it has been described that microcardia, a condition often observed in young children, appears as a consequence of severe fluid loss. However, the role of AQPs in this condition has not been fully explored. We have previously reported that our 3-day water restriction protocol in 25-day-old rats may be a useful animal model to explore microcardia [18]. Here, we show that NO system inhibition in dehydrated 25-day-old animals prevented the decrease in cardiomyocyte dimensions and water content, probably improving myocardial water balance, suggesting that both AQP1 and NO system may be involved in dehydration-induced microcardia.

On the other hand, in the 50-day-old R group, it was observed that water restriction induced the appearance of AQP1 in the plasma membrane accompanied by increased protein levels of this water channel, as previously reported [17]. This increase in AQP1 plasma membrane expression probably prevented changes in cardiomyocyte diameter and water content, further supporting our hypothesis that AQP1 contributes to cell volume regulation as previously mentioned. Moreover, NOS inhibition did not alter the

Table 2
Cardiac membrane vesicle diameters measured by dynamics light scattering.

	Control	$HgCl_2$	SNP	$HgCl_2$ + SNP
Vesicle diameter (nm)	341.6 ± 3.3	339.6 ± 2.1	340.2 ± 2.8	348.2 ± 3.6

Results are expressed as mean ± SD.

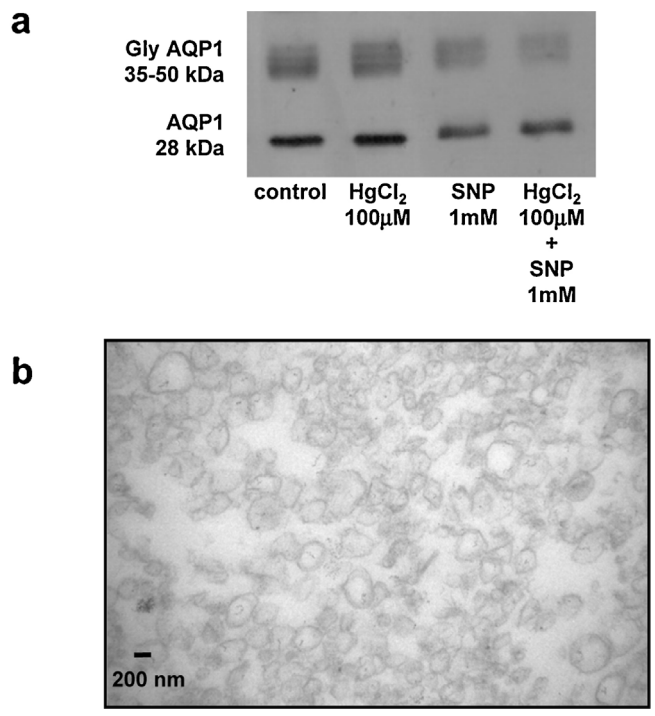

Fig. 6. Plasma membrane vesicles of cardiac tissue. Panel A: Representative western blots of AQP1 of membrane vesicles for each experimental condition. Panel B: Electron microscopy photograph of the obtained membrane vesicles (magnification X50000).

changes triggered by water restriction, suggesting that cardiac NO system is not involved in AQP1 regulation in this age group. These results are in agreement with the fact that ventricular NO production is not modified in during osmotic stress in this age group, as shown in Fig. 1. Surprisingly, AQP1 was decreased in the 50-day-old CL group. Recently, Mohammadi and Dehghani [24] reported that a low-dose L-NAME treatment caused a reduction of AQP1 transcription during brain ischemia/reperfusion. NO can regulate the expression of many genes, not only by a direct influence on the activity of transcription factors (TF) but also by modulation of upstream signaling cascades, mRNA stability and translation, as well as the processing of the primary gene products [25]. On the other hand, it has been reported that several TF such as NF-κB, HIF-1 y AP-1, are modified by S-nitrosylation [26].The mentioned TF have binding sites in AQP1 gene promoter [27]. Therefore, it is possible that changes in NO production may alter TF S-nitrosylation and consequently AQP1 expression, although further experiments are required to determine this. Moreover, considering that NO system inhibition decreased AQP1 protein levels in CL50 animals and osmotic stress increased its expression in R50 animals, we suggest that osmotic stress has more influence on AQP1 expression in comparison to NO system in 50-day-old animals. This may be explained, at least in part, by the fact that NO system activity decreases with postnatal growth and this may trigger the activation of other regulatory systems in this age group. It is interesting to notice that, despite the fact that NOS inhibition occurs in a similar percentage in L-NAME-treated animals of both ages, the hemodynamic response and changes in AQP1 localization and abundance are different in 25- and 50-day-old animals, suggesting that the effects of NO system inhibition are age related and probably have a different impact on the adaptation to hypovolemic state.

In the present work, results indicate that changes in AQP1 abundance and localization in response to osmotic stress may not influence BP regulation. Taking into account AQP1 mediated transport of NO described by Herrera et al. [6], regulatory mechanisms triggered by hypovolemic state that affect this water channel are likely to modify NO transport across cell membranes and therefore have an impact on cardiac or vascular function. In *in vitro* experiments, AQP1 knock-out mice presented decreased NO bioavailability and NO-dependent endothelial relaxation [7]. However, Montiel et al. [28] described that AQP1 knock-out mice presented decreased SBP without alterations in NO system functionality *in vivo*. Therefore, taking into account these controversial results, we continued to study the relationship between NO system and AQP1 in the heart by evaluating age-related differences in AQP1 S-nitrosylation during hypovolemic state and its effects on cardiac membrane vesicles osmotic water permeability. Results indicated that in the 50-day-old group, AQP1 S-nitrosylation did not change in response to water restriction. Taking into account that dehydrated animals from this age group showed an increase in AQP1 in cardiomyocyte plasma membrane without changes in cardiac NOS activity, it would be expected that NO system is not involved in AQP1 regulation. On the other hand, the 25-day-old R group, who presented an increase in cardiac NOS activity without changes in AQP1 abundance or localization, we observed a larger superposition of AQP1 and

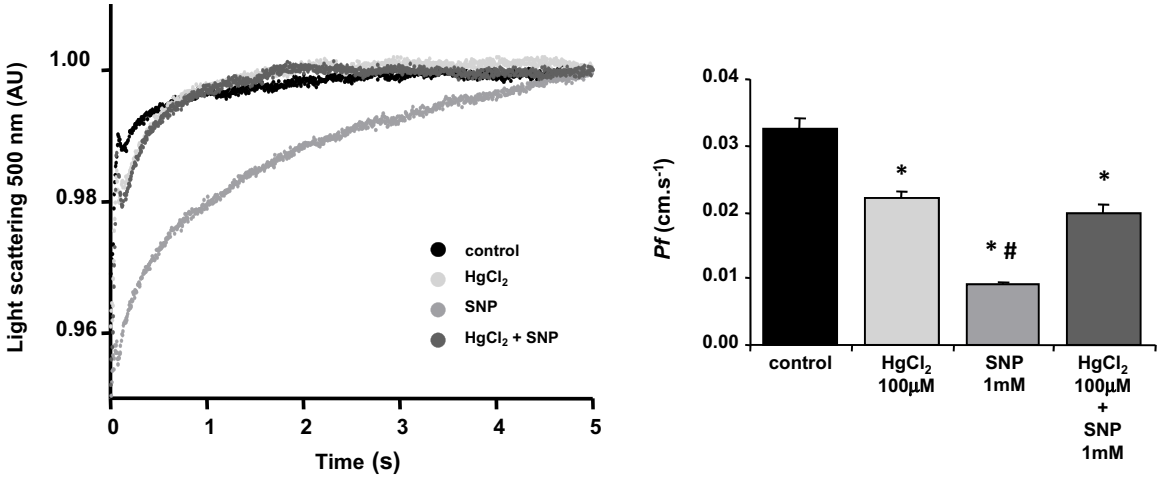

Fig. 7. Osmotic water permeability of plasma membrane vesicles of cardiac tissue. Panel A: Representative time-course of scattered light intensity at 500 nm followed by stopped-flow spectrometry. Panel B: *Pf* of plasma membrane vesicles of cardiac tissue. Data are expressed as mean ± SD. *$p < 0.05$ vs. control condition; #$p < 0.05$ vs. $HgCl_2$ treatment.

SNO-Cys signals, indicating that there may be a NO-dependent mechanism regulating water channel permeability. It has been reported that AQP1 S-nitrosylation in Cys189 blocks the passage of water through the channel pore [29,30]. Therefore, the present results suggest that this mechanism of water channel S-nitrosylation may participate in maintaining water homeostasis in the rat heart. As a last step, we set out the question of which would be the physiological effect of increased AQP1 S-nitrosylation on water permeability of cardiac membranes. Therefore, the osmotic water permeability coefficient of cardiac membrane vesicles was determined by stopped-flow spectrometry in the presence of NO donor SNP. This methodology allows the study of plasma membrane permeability in the absence of metabolic activity or cellular signaling mechanisms [21], which is difficult to achieve on the heart because of its tissue structure. First, vesicle size and morphology were assessed by DLS and EM and results indicated that vesicles were homogeneous and knowing their size allowed us to calculate *Pf*. Cardiac membrane vesicles in control conditions showed a high value of *Pf*, compatible with the presence of functional AQPs in the membrane [21], also considering that water transport was inhibited by 30% by $HgCl_2$ treatment, an AQP inhibitor by interaction with SH group of Cys189 in the constriction site of AQP1 channel pore [31]. In the rabbit heart, it was reported that AQPs contribute to a similar percentage to membrane *Pf* by using AQP inhibitors [32]. In isolated myocytes, lower *Pf* values were reported, probably because the contribution of endothelial AQPs was excluded [33,34]. Even though the experimental model applied in these experiments estimates *Pf* from cardiomyocyte membrane and endothelial cells membrane, the amount of endothelial cells is considerably less than cardiomyocyte cells in the heart. Cardiac membrane vesicles treated with SNP showed a decreased *Pf*, indicating that NO may affect cardiac membrane water permeability. Interestingly, Schluter et al. [35] reported that the increase in osmotic fragility experienced by isolated cardiomyocytes after reoxygenation could be prevented by NO donors by a cGMP-independent mechanism. Results from the present study may explain, at least in part, those results. As previously mentioned, in the rat heart, AQP1 is the most abundant and functionally relevant AQP [2]. Even though a more appropriate control to assure that AQP1 is involved in the observed changes in water permeability is the use of small interfering RNAs (siRNA) to induce the short-term silencing of proteins, we suggest that AQP1 S-nitrosylation may be the responsible mechanism for the observed changes in *Pf* induced by SNP *in vitro*. Moreover, because of the observed decrease in water permeability, SNP may also alter other AQPs or plasma membrane properties. It should be outlined that because of the experimental design, results obtained with SNP treatment are a consequence of its interaction with plasma membrane and its proteins and not other processes such as protein internalization or trafficking. Additionally, the time scale of these experiments does not allow studying those processes. On the other hand, the inhibition of SNP-induced changes in *Pf* by simultaneous Hg^{2+} treatment, which binds specifically to Cys residues, may support the hypothesis of AQP1 and SNP interacting by S-nitrosylation of Cys189. It has been reported that Hg^{2+} can decompose S-nitrosotioles by Saville reaction, where mercury replaces SNO group united to a thiol group [36,37]. Therefore, it is possible that Hg^{2+} prevents or disrupts AQP1 S-nitrosylation by reacting with thiol groups of Cys and causing *Pf* to be similar to $HgCl_2$ treatment. Altogether, water permeability measurements provide evidence to explain the reduction in cardiomyocyte diameter and cardiac water content observed in R 25-day-old rats, as reduced P*f* because of increased AQP1 S-nitrosylation may affect the ability of cardiac cells to regulate their volume after 3 days of dehydration, as previously explained.

In conclusion, the present results provide evidence to support a role of NO system in the age-related modulation of AQP1 abundance and localization on cardiac tissue. In the 25-day-old animals, NO system inhibition may alter cardiac AQP1 plasma membrane localization during osmotic stress, which is associated to the maintenance of cellular dimensions and cardiac water content, supporting a role of AQP1 in long-term cell volume regulation. Increased AQP1 S-nitrosylation in the 25-day-old group, which may induce a decrease in *Pf*, could explain the more severe alterations in water homeostasis during hypovolemic state. On the other hand, in the 50-day-old rats, NO system may not be involved in the regulation of AQP1 abundance or localization during osmotic stress. Water transport inhibition induced by NO donor may influence cardiac water homeostasis during physiological or physiopathological states when there may be an increase in NO production. Altogether these findings add new insights into the knowledge of age-related AQP1 regulation in the heart and may provide future targets for therapy.

Conflict of interest

The authors declare no conflict of interest.

Acknowledgements

This study was supported by the University of Buenos Aires, Argentina, Grant 20020100100068. The authors wish to thank Katia Seremeta and Dr. Alejandro Sosnik (Cátedra de Farmacotecnia, Facultad de Farmacia y Bioquímica, Universidad de Buenos Aires) for DLS measurements of plasma membrane vesicles, Dr. Juan José Lopez-Costa (Instituto de Biología Celular y Neurociencia "Prof. E. De. Robertis", Facultad de Medicina, Universidad de Buenos Aires) for electron microscopy photographs and Dr. Mónica Montes and Dr. Rolando Rossi (Instituto de Química y Fisicoquímica Biológicas, Facultad de Farmacia y Bioquímica, Universidad de Buenos Aires) for stopped flow measurements.

Appendix A. Supplementary data

Supplementary data associated with this article can be found, in the online version, at http://dx.doi.org/10.1016/j.biopha.2016.03.050.

References

[1] A.S. Verkman, A.K. Mitra, Structure and function of aquaporin water channels, Am. J. Physiol. Renal Physiol. 278 (2000) F13–F28.
[2] T. Butler, C. Au, B. Yang, J. Egan, Y. Tan, E.C. Hardeman, K.N. North, A.S. Verkman, D.S. Winlaw, Cardiac aquaporin expression in humans rats, and mice, Am. J. Physiol. Heart Circ. Physiol. 291 (2006) H705–H713, doi:http://dx.doi.org/10.1152/ajpheart.00090.2006.
[3] R.T. Miller, Aquaporin in the heart—only for water? J. Mol. Cell. Cardiol. 36 (2004) 653–654.
[4] V. Endeward, R. Musa-Aziz, G.J. Cooper, L.M. Chen, M.F. Pelletier, L.V. Virkki, C.T. Supuran, L.S. King, W.F. Boron, G. Gros, Evidence that aquaporin 1 is a major pathway for CO2 transport across the human erythrocyte membrane, FASEB J. 20 (2006) 1974–1981, doi:http://dx.doi.org/10.1096/fj.04-3300com.
[5] T. Litman, R. Søgaard, T. Zeuthen, Ammonia and urea permeability of mammalian aquaporins, Handb. Exp. Pharmacol. 190 (2009) 327–358, doi:http://dx.doi.org/10.1007/978-3-540-79885-9_17.
[6] M. Herrera, N. Hong, J.L. Garvin, Aquaporin-1 transports NO across cell membranes, Hypertension 48 (2006) 157–164, doi:http://dx.doi.org/10.1161/01.HYP.0000223652.29338.77.
[7] M. Herrera, J.L. Garvin, Novel role of AQP-1 in NO-dependent vasorelaxation, Am. J. Physiol. Renal Physiol. 292 (2007) 1443–1451, doi:http://dx.doi.org/10.1152/ajprenal.00353.2006.
[8] G.J. Cooper, Y. Zhou, P. Bouyer, I. Grichtchenko, W.F. Boron, Transport of volatile solutes through AQP1, J. Physiol. 542 (2002) 17–29, doi:http://dx.doi.org/10.1113/jphysiol.2002.023218.
[9] S.P. Tsunoda, B. Wiesner, D. Lorenz, W. Rosenthal, P. Pohl, Aquaporin-1, nothing but a water channel, J.Biol. Chem. 279 (2004) 11364–11367, doi:http://dx.doi.org/10.1074/jbc.M310881200.

[10] A.S. Verkman, Does aquaporin-1 pass gas? An opposing view, J. Physiol. 542 (2002) 31, doi:http://dx.doi.org/10.1113/jphysiol.2002.024398.
[11] M. Herrera, J.L. Garvin, Aquaporins as gas channels, Pflugers Arch. 462 (2011) 623–630, doi:http://dx.doi.org/10.1007/s00424-011-1002-x.
[12] N. Arreche, A. Fellet, M. López, J.J. López-Costa, C. Arranz, A.M. Balaszczuk, Hypovolemic state: involvement of nitric oxide in the aged related alterations of aquaporin-2 abundance in rat kidney, Vascul. Pharmacol. 49 (2008) 19–25, doi:http://dx.doi.org/10.1016/j.vph.2008.04.001.
[13] K. Nagai, M. Watanabe, M. Seto, A. Hisatsune, T. Miyata, Y. Isohama, Nitric oxide decreases cell surface expression of aquaporin-5 and membrane water permeability in lung epithelial cells, Biochem. Biophys. Res. Commun. 354 (2007) 579–584, doi:http://dx.doi.org/10.1016/j.bbrc.2007.01.026.
[14] A. Martínez-Ruiz, S. Lamas, S-nitrosylation: a potential new paradigm in signal transduction, Cardiovasc. Res. 62 (2004) 43–52, doi:http://dx.doi.org/10.1016/j.cardiores.2004.01.013.
[15] D.R. Gonzalez, A. Treuer, Q.A. Sun, J.S. Stamler, J.M. Hare, S-Nitrosylation of cardiac ion channels, J. Cardiovasc. Pharmacol. 54 (2009) 188–195, doi:http://dx.doi.org/10.1097/FJC.0b013e3181b72c9f.
[16] M. Kadekaro, G. Su, R. Chu, Y. Lei, J. Li, L. Fang, Effects of nitric oxide on expressions of nitrosocysteine and calcium-activated potassium channels in the supraoptic nuclei and neural lobe of dehydrated rats, Neurosci. Lett. 411 (2007) 117–122, doi:http://dx.doi.org/10.1016/j.neulet.2006.10.035.
[17] V.A. Netti, M.C. Vatrella, M.F. Chamorro, M.I. Rosón, E. Zotta, A.L. Fellet, A.M. Balaszczuk, Comparison of cardiovascular aquaporin-1 changes during water restriction between 25- and 50-day-old rats, Eur. J. Nutr. 53 (2014) 287–295, doi:http://dx.doi.org/10.1007/s00394-013-0527-5.
[18] V.A. Netti, A.N. Iovane, M.C. Vatrella, N.D. Magnani, P.A. Evelson, E. Zotta, A.L. Fellet, A.M. Balaszczuk, Dehydration affects cardiovascular nitric oxide synthases and caveolins in growing rats, Eur. J. Nutr. (2015), doi:http://dx.doi.org/10.1007/s00394-014-0820-y.
[19] A. Stoessel, A. Paliege, F. Theilig, F. Addabbo, B. Ratliff, J. Waschke, D. Patschan, M.S. Goligorsky, S. Bachmann, Indolent course of tubulointerstitial disease in a mouse model of subpressor, low-dose nitric oxide synthase inhibition, Am, J. Physiol. Renal Physiol. 295 (2008) F717–725, doi:http://dx.doi.org/10.1152/ajprenal.00071.2008.
[20] F.B. Ding, Y.M. Yan, J.B. Huang, J. Mei, J.Q. Zhu, H. Liu, The involvement of AQP1 in heart oedema induced by global myocardial ischemia, Cell. Biochem. Funct. 31 (2013) 60–64, doi:http://dx.doi.org/10.1002/cbf.2860.
[21] A.S. Verkman, Water permeability measurement in living cells and complex tissues, J. Membrane Biol. 173 (2000) 73–87, doi:http://dx.doi.org/10.1007/s002320001009.
[22] M.B. Burg, J.D. Ferraris, N.I. Dmitrieva, Cellular response to hyperosmotic stresses, Physiol. Rev. 87 (2007) 1441–1474.
[23] M.T. Conner, A.C. Conner, C.E. Bland, L.H. Taylor, J.E. Brown, H.R. Parri, R.M. Bill, Rapid aquaporin translocation regulates cellular water flow: mechanism of hypotonicity-induced subcellular localization of aquaporin 1 water channel, J. Biol. Chem. 287 (2012) 11516–11525, doi:http://dx.doi.org/10.1074/jbc.M111.329219.
[24] M.T. Mohammadi, G.A. Dehghani, Nitric oxide as a regulatory factor for aquaporin-1 and 4 gene expression following brain ischemia/reperfusion injury in rat, Pathol. Res. Pract. 211 (2014) 43–49, doi:http://dx.doi.org/10.1016/j.prp.2014.07.014.
[25] C. Bogdan, Nitric oxide and the regulation of gene expression, Trends Cell. Biol. 11 (2001) 66–75, doi:http://dx.doi.org/10.1016/S0962-8924(00)01900-0.
[26] Y. Sha, H.E. Marshall, S-nitrosylation in the regulation of gene transcription, Biochim. Biophys. Acta 1820 (2012) 701–711, doi:http://dx.doi.org/10.1016/j.bbagen.2011.05.008.
[27] I. Abreu-Rodríguez, R. Sánchez Silva, A.P. Martins, G. Soveral, J.J. Toledo-Aral, J. López-Barneo, M. Echevarría, Functional and transcriptional induction of aquaporin-1 gene by hypoxia; analysis of promoter and role of Hif-1α, PLoS One 6 (2011) e28385, doi:http://dx.doi.org/10.1371/journal.pone.0028385.
[28] V. Montiel, E. Leon Gomez, C. Bouzin, H. Esfahani, R. Romero Perez, I. Lobysheva, O. Devuyst, C. Dessy, J.L. Balligand, Genetic deletion of aquaporin-1 results in microcardia and low blood pressure in mouse with intact nitric oxide-dependent relaxation, but enhanced prostanoids-dependent relaxation, Eur. J. Physiol. 466 (2014) 237–251, doi:http://dx.doi.org/10.1007/s00424-013-1325-x.
[29] G. Lahajnar, S. Pecar, A. Sepe, Na-nitroprusside and HgCl2 modify the water permeability and volume of human erythrocytes, Bioelectrochemistry 70 (2007) 462–468, doi:http://dx.doi.org/10.1016/j.bioelechem.2006.07.009.
[30] G. Lahajnar, B. Sobotič, A. Sepe, V. Jazbinšek, S. Pečar, Influence of sodium nitroprusside on human erythrocyte membrane water permeability: an NMR study, Gen. Physiol. Biophys. 29 (2010) 373–380, doi:http://dx.doi.org/10.4149/gpb_2010_04_373.
[31] G. Preston, J. Jung, W. Guggino, P. Agre, The mercury-sensitive residue at cysteine 189 in the CHIP28 water channel, J. Biol. Chem. 268 (1993) 17–20.
[32] M.R. Kellen, J.B. Bassingthwaighte, An integrative model of coupled water and solute exchange in the heart, Am. J. Physiol. Heart Circ. Physiol. 285 (2003) H1303–H1316, doi:http://dx.doi.org/10.1152/ajpheart.00933.2001.
[33] T. Ogura, S. Imanishi, T. Shibamoto, Osmometric and water-transporting properties of guinea pig cardiac myocytes, Jpn. J. Physiol. 52 (2002) 333–342, doi:http://dx.doi.org/10.2170/jjphysiol.52.333.
[34] M.A. Suleymanian, C.M. Baumgarten, Osmotic gradient-induced water permeation across the sarcolemma of rabbit ventricular myocytes, J. Gen. Physiol 107 (1996) 503–514.
[35] K.D. Schlüter, G. Jakob, M. Ruiz-Meana, D. Garcia-Dorado, H.M. Piper, Protection of reoxygenated cardiomyocytes against osmotic fragility by nitric oxide donors, Am. J. Physiol. 271 (1996) H428–434.
[36] P.T. Doulias, K. Raju, J.L. Greene, M. Tenopoulou, H. Ischiropoulos, Mass spectrometry-based identification of S-nitrosocysteine in vivo using organic mercury assisted enrichment, Methods 62 (2013) 165–170, doi:http://dx.doi.org/10.1016/j.ymeth.2012.10.009.
[37] H.R. Swift, D.L.H. Williams, Decomposition of S-nitrosothiols by mercury(II) and silver salts, J. Chem. Soc. Perkin. Trans 2 (1997) 1933–1935, doi:http://dx.doi.org/10.1039/A702937C.